



Performance Enhancement the Gas Turbines of Power Plants by using Tilt Bearings Development

Alaa Jasim Abdulah^{1,*}, Hashim A.Hussien¹, Abdul Jabbar Owaid¹

¹ University of Technology, Elctromechnical Eng. Dep., Baghdad, Iraq

ARTICLE INFO	ABSTRACT
<p>Article history: Received 20 July 2025 Received in revised form 29 November 2025 Accepted 10 December 2025 Available online 11 January 2026</p> <p>Keywords: Gas turbine; transient analysis; harmonic analysis; tilt-bearing; vibration; modal analysis; deformation</p>	<p>The gas turbine in Power Plants is an internal combustion engine that transforms liquid fuels into mechanical energy. The gas turbine frequently produces exaggerated vibrations or noise. This work aims to replace the type of bearing with a tilt-bearing kind with a mechanical damper and numerically replicate the process by creating a depression in the bearing pad to improve the oil's flow and reduce the generated vibration. The ANSYS application employed the finite element approach during the analysis phase. The analytical simulation to execute a dynamic analysis system for gas turbines proposed two cases before and after the development, simulating and comparing the outcomes of the cases. Following the adjustments, the system's deformation value dropped to 46.17%, its stress value dropped to 39.66%, and its strain value dropped to 61.47%. The harmonic analysis revealed that the deformation value fell to 38.18%.</p>

1. Introduction

The air compressor, combustion chamber, and turbine constitute the fundamental constituents of the gas unit, utilized in power plants. Studies have indicated that each portion experiences the above-stated mechanical vibrations at a different part[1]. For the parametric ID method that uses real-time operating data and the (ARMAX) methodology to monitor the characteristics of vibration of bearings used in the MS5002B gas turbine [2], an attempt was made to relate the findings of the research on the turbine's vibrational field, including the stand, to the impact of the turbine test stand's components. In both stationary and transient test mode [3], the primary function of the gas turbine blade is to rotate the shaft attached to the generator motor. Gas turbine blades in power plants are subjected to extreme pressure, vibration, and temperature; thus, the materials used in their fabrication must be able to withstand these challenging operating conditions [4]. An innovative 3D thermo-hydrodynamic model incorporates the mass conservation principles to enhance the precision and comprehensiveness of prognostications pertaining to the vibrational characteristics of oil scarcity in the presence of varying rotor imbalances and lubricating oil cooling circumstances. By

Corresponding author
E-mail address: eme.19.18@uotechnology.edu.iq

<https://doi.org/10.37934/sej.12.1.4761>

manipulating the oil inflow rate and temperature at the entrance of the groove, the newly devised model approximates the pressure and oil concentration [5]. A variety of techniques have already been presented to identify structural deterioration based on modifications in modal parameters. The frequency change ratio of the two modes is used as a damage indicator [6]. Certain research in numerical investigation takes the cavitation effects into account [7]. The adverse impact on the performance of the compressor is caused by the tip clearance that exists between its rotating blades and the casing. This clearance leads to a loss of energy [8]. The factors considered were the effect of genuine reverberation, the parameters of bearing clearances, arrangement, and unbalance. The application of the standard approach proved to be highly efficient in terms of time saved, leading to enhanced outcomes [9]. The elements of the gas turbine are examined and demonstrated utilizing a powerful nonlinear autoregressive methodology with outer exogenous information (NARX) [10]. The most generally announced causes portrayed are that can deliver damaging vibration in the gas turbine of CCPs, for example, unbalancing and misalignment, contact among pivoting and fixed parts (scouring), steam stream vacillations, the basic rotor speed, and shorted turns [11]. A mathematical model of the stand and a calculation algorithm that allow one to construct the transfer function of the stand's element base and link the conditions for a possible change in the wave field with the results of measuring the parameters of the turbine operation as part of the stand must be developed [3]. The reason for this approach is to further develop constant observing capacity with the utilization of present-day ID calculations, guaranteeing reliable and safe activity in power-age plants [12]. In many industrial settings, gas turbines are necessary for producing electricity as well as for the propulsion of trains, ships, and airplanes [13]. The presentation corruption of a heavy-duty gas turbine under base load and various intermediate loads was replicated [14, 15]. Three-dimensional finite element models were built using CATIA and analyzed by ANSYS WORKBENCH, and a weighted-sum approach was employed to solve the multi-objective optimization problem. Mansoor *et al.*, [16] demonstrated that the multitude of goals that must be achieved in a typical gas turbine study. The initial goal is to anticipate the natural frequencies and determine the turbine system's mode shapes at those frequencies. To determine the critical speeds inside or near a rotor system's working speed range, performing an unbalanced response investigation on a gas turbine is essential in order to ascertain the displacement of the rotor. Additionally, it is imperative to gauge the forces exerted on the rotor, which may arise due to a rotor imbalance. Furthermore, a comprehensive analysis of operational concerns and potential capacity risks associated with the rotor dynamics of a specific rotor system should be conducted. Two primary forms of instabilities, namely surge and stalls, frequently manifest in the systems of compressors that impact the gas turbines [17]. The objective of this research is to select the appropriate groove for tilt bearings to increase the oil flow rate, thereby reducing the occurrence of vibrations in the gas turbine system and the main aim of this work is to improve the performance of gas turbine through reducing the vibrations emphasis on the rotor as well as the shaft-disk-blade. The innovation in this work is testing the modifications made to tilt bearings by creating grooves on the entire gas turbine system through simulation. The analysis was not limited to just the tilt bearing part.

2. Governing Equation

Pivoting circles are a pragmatic concern in many fields of design, for example, mechanical, marine, and aviation businesses, including gas turbine motors, like turbojet, turbofan, turboprop, and super shaft motors; gears; turbo machinery; flywheel frameworks; super siphons; super generators; and outward blowers. For a better comprehension of the behavior and the most effective design of rotors, it is essential to conduct an analysis of the distribution of stress and strain in high-speed

rotating disks of variable thickness [18]. When designing rotating machinery, it is crucial to take into account its dynamic properties to prevent catastrophic failures caused by resonance conditions during the operation. Numerous researchers have studied the dynamics of rotating machinery and turbo machinery rotors, and in recent years, a large number of researchers have become interested in the FEM as an efficient numerical technique for studying the dynamics of mechanical structures and rotating equipment [19], fostered a FEM to concentrate on the powerful qualities of single-rotor and double-rotor bearing super hardware frameworks. Natural frequency predictions, critical speed maps, and an estimate of bearing stiffness were all derived from the model's analysis. They demonstrated that the velocity proportion between the fast and low-speed shafts of the double rotor can be utilized as one of the plan boundaries of the double rotor framework [20]. The following formula displays the vibration signal [21]:

$$x(t) = A \cdot \sin(\omega t + \phi) \quad (1)$$

Differentiating the vibration expression in Equation (1) yields the speed of vibration, denoted as $v(t)$, which is represented by Equations (2), whereas the acceleration of vibration, denoted as $a(t)$, is represented by Equations (3).

$$v(t) = \frac{dx(t)}{dt} = A\omega \cos(\omega t + \phi) \quad (2)$$

$$a(t) = \frac{dv(t)}{dt} = -A\omega^2 \sin(\omega t + \phi) \quad (3)$$

The Brayton cycle is connected to the energy evaluation of the gas turbine cycle. Evaluations of the system's input and output energy will be a part of the computation. The essential parts of the gas turbine cycle incorporate air blowers, an ignition chamber, and the gas turbine. The followings are the conditions expected for dissecting each part of the gas turbine cycle [22].

2.1 Compressor:

$$r_1 = r_1 \left(1 + \frac{1}{\pi_{xi}} \left(r_{xi}^{\frac{N}{\gamma}} - 1 \right) \right) \quad (4)$$

$$W_{Ac} = m_a \zeta_0 (T_2 - T_1) \quad (5)$$

$$\rho_{p\mu}(T) = 1.048 - \left(\frac{1.837}{10^4} \right) + \left(\frac{9.45T^3}{10^7} \right) - \left(\frac{5.49T^7}{10^{29}} \right) + \left(\frac{7.92T^4}{10^{14}} \right) \quad (6)$$

Equation (4) shows the specific heat ratio (γ), the compression ratio (r), and the air temperatures at the compressor's input and discharge sections denoted by T_1 and T_2 , respectively. Equation (5) is utilized to ascertain the blower's power consumption. Depending on the varying temperatures, equation (6) provides the air's particular heat.

2.2 Combustion chamber:

$$\dot{m}_a h_2 + \dot{m}_f LHV = \dot{m}_\beta h_3 + (1 - \eta_{cc}) \dot{m}_f LHV \quad (7)$$

$$\dot{m}_g = \dot{m}_f + \dot{m}_a \quad (8)$$

$$f = \frac{\dot{m}_f}{\dot{m}_a} \quad (9)$$

2.3 Gas turbine:

$$T_4 = T_3 \left(1 - n_{GT} \left(1 - \left(\frac{P_3}{P_4} \right)^{\frac{k-1}{k}} \right) \right) \quad (10)$$

$$\dot{W}_{GT} = m_g C_{mg} (T_{A_3} - T_{A_4}) \quad (11)$$

$$C_{1N}(T) = 0.991 + \left(\frac{6.997T}{10^5} \right) + \left(\frac{2.712T^2}{10^7} \right) - \left(\frac{1.2244T^3}{10^{10}} \right) \quad (12)$$

Considering a cylindrical bearing of radius R and thickness t, we can start by expressing the radial displacement (u_r) and axial displacement (u_a) as functions of the cylindrical coordinates (r , θ , and z) and time (t). These displacements describe how the bearing deforms under the applied loads.

Using the theory of linear elasticity, we can derive the following equations for the radial and axial strains (ε_r , ε_a) [23]:

$$\begin{aligned} \varepsilon_r &= \frac{1}{R} \frac{\partial u_r}{\partial r} + \frac{u_r}{R} \\ \varepsilon_a &= \frac{\partial u_a}{\partial z} \end{aligned} \quad (13)$$

The equilibrium equations for the bearing. In the absence of a be expressed as[24]:

$$\begin{aligned} \frac{1}{r} \frac{\partial}{\partial r} (r \sigma_r) + \frac{\partial \sigma_\theta}{\partial \theta} + \frac{\partial \sigma_{rz}}{\partial z} &= 0 \\ \frac{\partial \sigma_a}{\partial z} + \frac{\partial \sigma_{az}}{\partial a} &= 0 \end{aligned} \quad (14)$$

Here ∂r , $\partial \theta$ and represent the radial and tangential stresses, while σ_{rz} , σ_{az} represent the shear stresses. These stresses are related to the strains through the constitutive equations of the material. The constitutive equations for an isotropic material, within the elastic limit, can be expressed as[25]:

$$\begin{aligned} \sigma_r &= (1 - \nu) D_r \varepsilon_r - \nu D_e \varepsilon_a \\ \sigma_a &= (1 - \nu) D_a \varepsilon_a - \nu D_r \varepsilon_r \\ \sigma_\theta &= \frac{D_r D_a}{D_r - E_a} (\varepsilon_r + \varepsilon_a) \\ \sigma_{rz} &= \tau_{rz} = G_{rz} \gamma_{rz} \\ \sigma_{az} &= \tau_{az} = G_{az} \gamma_{az} \end{aligned} \quad (15)$$

Here, ν represents Poisson's ratio, E_r and E_a are the radial and axial moduli of elasticity, and G_{rz} and G_{az} represent the shear moduli in the radial and axial directions, respectively. Finally, γ_{rz} and γ_{az} denote the corresponding shear strains.

Turbine component subjected to mechanical loads. The following equations can be employed:

Equilibrium equations[27]:

$$\begin{aligned} \frac{\partial \sigma_z}{\partial z} + \frac{\partial \sigma_{zy}}{\partial y} + F_x &= 0 \\ \frac{\partial \sigma_z}{\partial x} + \frac{\partial \sigma_m}{\partial y} + F_y &= 0 \end{aligned} \quad (16)$$

Here, Here, σ_{xx} , σ_{yy} , and σ_{xy}) denote the components of stress in the x and y directions. F_x , F_y represent the applied mechanical forces.

Constitutive equations [26]:

$$\begin{aligned}\sigma_{xx} &= E \cdot \epsilon_{xx} + \nu \cdot E \cdot \epsilon_{yy} \\ \sigma_{yy} &= \nu \cdot E \cdot \epsilon_{xx} + E \cdot \epsilon_{yy} \\ \sigma_{xy} &= 2G \cdot \gamma_{xy}\end{aligned}\tag{17}$$

Here, E represents the modulus of elasticity, ν is Poisson's ratio, and (G) stands for the shear modulus. ϵ_{xx} and ϵ_{yy} are the components of strain in the x and y directions, while γ_{xy} represents the shear strain.

Compatibility equation[25]:

$$\frac{\partial^2 u}{\partial x^2} + \frac{\partial^2 v}{\partial y^2} + \frac{\partial^2 w}{\partial z^2} = 0\tag{18}$$

This compatibility equation, which accounts for the deformation compatibility between different directions, ensures a physically valid deformation field. u and v represent the displacements in the x and y directions, while w denotes the out-of-plane displacement (if applicable).

3. Geometry and Modeling

Solid works 2018 was used to show the whole parts of the gas turbine. The parts of the gas turbine were downloaded and utilized in Solid works programming to do the math. To create scale with the captures, the Solid works assembly extension assembles many of the model's 38 components. The sharp edges were thought to be one circle in each stage, since, in such a case, every one of the sharp edges that will make numerous components in the lattice that are consuming most of the day to tackle in Ansys was utilized or modeled. There are three kinds of bearings utilized in the primary model, as well as two dampers used to further develop and review the performance. A model made with expel is separated into three sections with a split element to represent distinct materialistic for each section (carbon steel, copper compound, and white metal). A replica of the gas turbine is displayed in Figure 1.

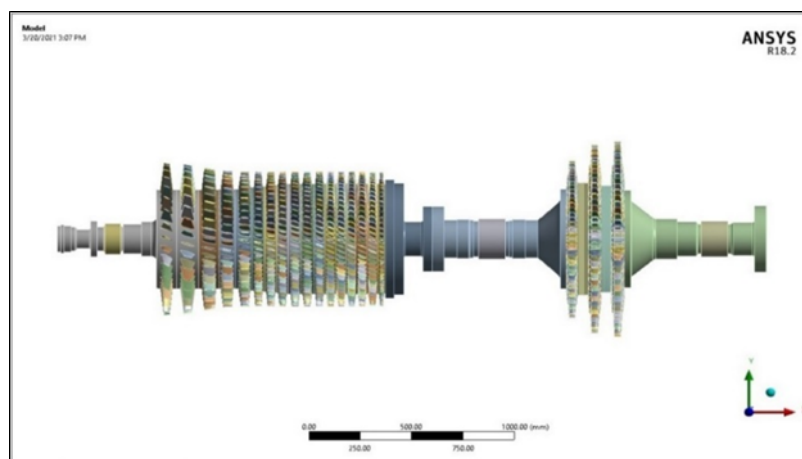


Fig. 1. Model of gas turbine with blades

4. Mathematical Methodology

In anticipating the actual way of designs and frameworks behaving, the limited component strategy (FEM) is the most well-known reenactment method. Since the experimental arrangements are regularly impractical in the design sciences for most day-to-day issues, mathematical methodologies were created to track down an answer for the specific issues' overseeing recipes [23]. In the examination, a three-layered model was employed. Using Solid Works 2018, the model was made. The program Ansys 18.2 was used to import the gas turbine development model's blade and apply the different FEM processes. First, tetrahedral components were used to discretize the turbine cutting edges for the unstructured body. The sharp edges and bends of the cutting edge were accommodated by the tetrahedral network. The entire number of hubs and components is 208074 and 114600, as displayed in figure 2. It makes sense that the work moves toward making a model for the soldering program's gas turbine. And afterward, the most common way of sending out the model to the ANSYS R18.2 program is with the end goal of examination and getting the outcomes. The limitation condition is displayed in Table I.

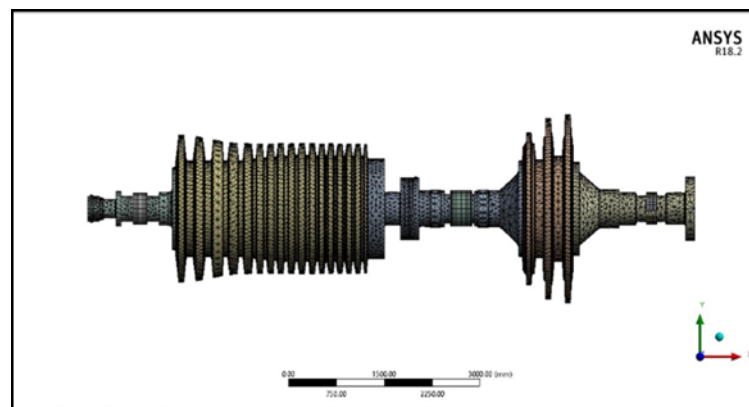


Fig. 2. Meshed geometry using ANSYS

Table 1

Limitation situation [1]

Parameters	Power in Action	Temperature of Turbines	Air compressor's exit pressure	Pressure in Turbines
Value	129.22 (MW)	1023 °C	1011 (kPa)	1011.8 (kPa)

5. Results

5.1 Case One (before development)

5.1.1 Free vibration

The gas turbine was made as math in the reenactment for simplicity of arrangement, with the complete twisting around (1.3124 mm) at recurrence (12.7716 Hz) for the first mode displayed in figure 3. The complete misshaping (2.8899 mm) at recurrence (51.488 Hz) for the second mode is evinced in figure 4. All designs have normal vibration frequencies at which they will deform, called reverberation. Each regular recurrence has an unsettling mode, a form that depicts the deformity of the design. The fundamental mode is the least frequent repetition at which misshaping occurs. The primary mode refers to the way a construction will work with the surrounding vibrating structures, or how it systematically describes the biggest stresses in a design.

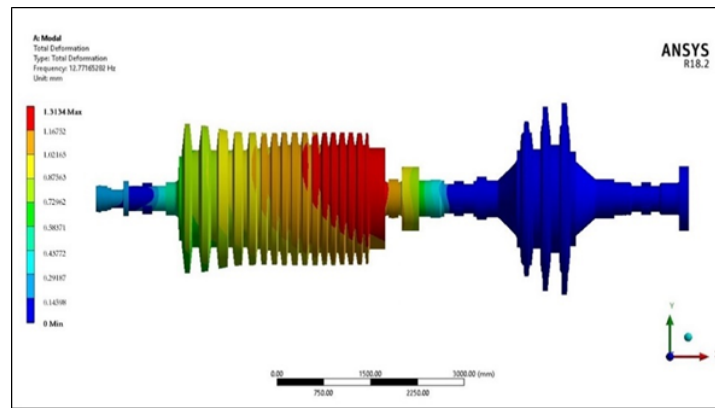


Fig. 3.12.77 Hz is the frequency of deformation. For the first mode

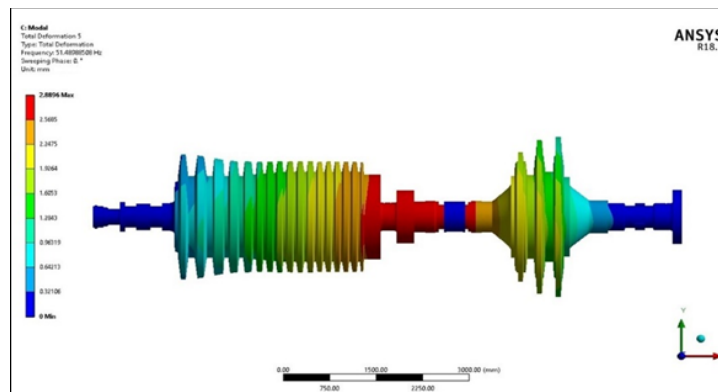


Fig. 4.51.48 Hz is the frequency of deformation. Regarding the second mode

5.1.2 Transient analysis

The largest amount of deformation, 2.238 mm, is elucidated in Figure 5. Additionally, Figure 6 illustrates the deformation's amplitude. The variation with time reached its maximum deformation value; the system reached stability after 53.5 seconds, used to ascertain a structure's dynamic reaction to a load that varies over time. Because of the temporal setting of this set of analyses, the damping effects of the structure are deemed significant. Figure 7 portrays the strain value of 0.0122 for the material with an analogous elastic modulus, whereas Figure 8 shows the value of stress (1128.3 MPa) obtained using the Von Mises technique with the same material.

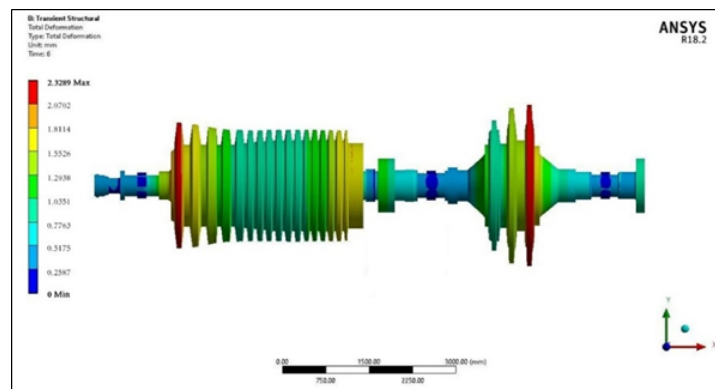


Fig. 5. Transient structure (Total deformation)

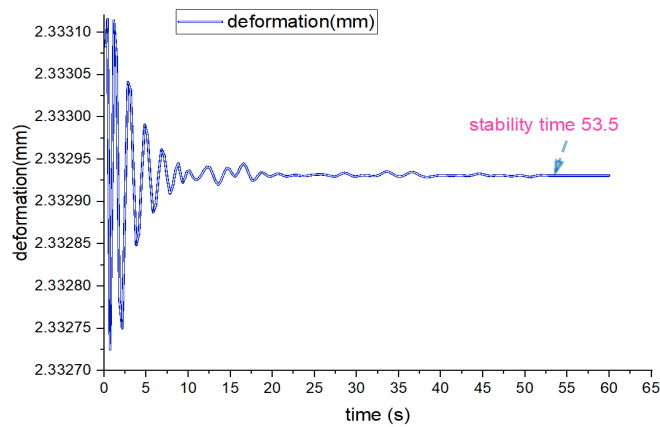


Fig. 6. Time affects the deformation's amplitude value

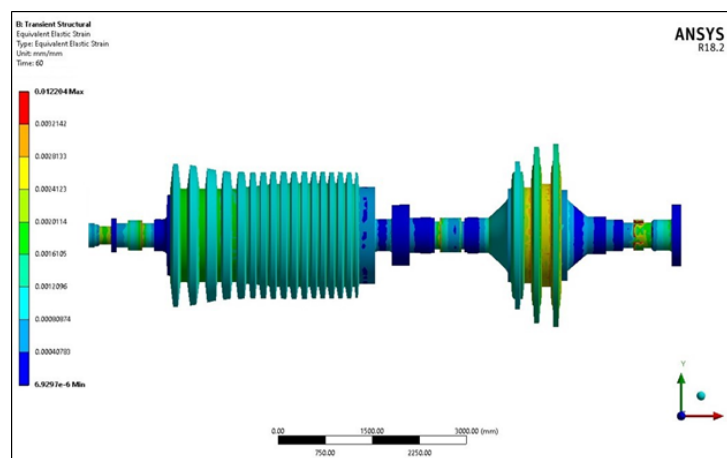


Fig. 7. The value of equivalent elastic strain

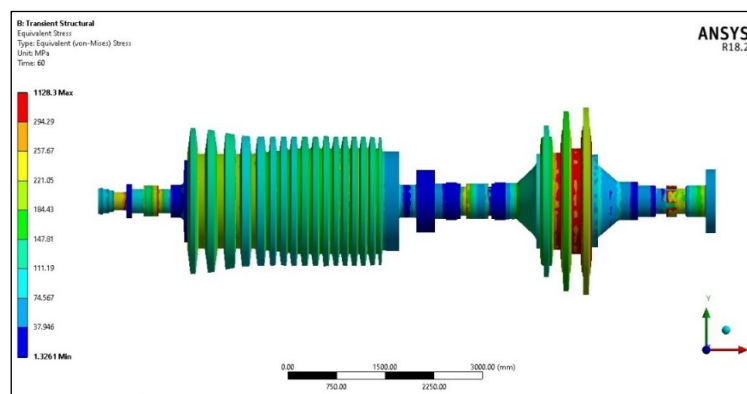


Fig. 8. The value of Stress for comparable material as determined by the Von Mises technique

5.1.3 Harmonic analysis (Forced vibration)

Figure 9 reveals the harmonic response's total deformation, or 2.2 mm, at a frequency of 50 Hz, whereas Figure 10 demonstrates the vibration's amplitude, altering on a regular basis. The vibration amplitude at 50 Hz has a greater value (2.3). The structure's steady-state response to cyclic stresses was examined. Determining a structure's dynamic reaction under larger, broader, time-dependent pressures is known as transient analysis.

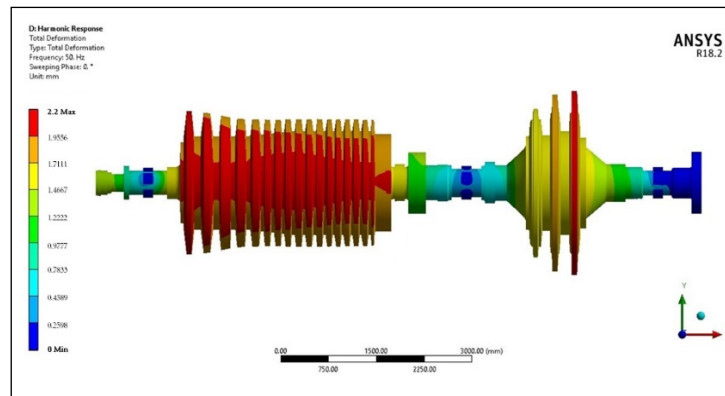


Fig. 9. Response of harmonic vibration at 50 Hz frequency

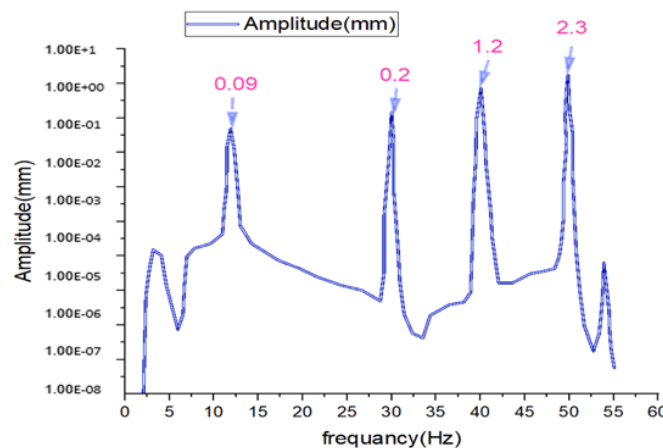


Fig. 10. The Frequency with Vibration value of Amplitude

5.2 Case two (after revisions)

The gas turbine vibration control system has been modified in:

- Due to their superior stability capabilities, the system's bearings were changed to tilt-pad bearings. Slant cushion heading produces tiny undermining cross-coupled solidity regardless of math, speed, load, or working inconsistency. Table II lists the bearing's material properties.
- Mechanical dampers are used under the foundation of the gas turbine framework. Which is a typical answer for diminishing how much vibration happens in the framework.
- Grooves (the Triple inclined) were implemented in the cushions as displayed in figures 11 and 12, where the pace of vibration for the gas turbine framework expanded, a more prominent measure of oil would be siphoned, and these furrows were made to retain this overabundance measure of oil, as well as it is realized that the oil can ingest vibrations. Table III displays the components of the cushion groove. The effective activity of the gas turbine and its determined hardware generally relies on the grease framework. As a result, the system as a whole need to be well maintained, and all factors that contribute to proper lubrication must be present. The oil type utilized in lubrication is significant because the assistance life of the gear relies upon the persistent lubricants of ointments of fitting quality, amount, temperature, and tension. In this situation, the life and nature of ointments are of imperative significance to clients. The grease-up oil used for this point is an enemy of rust and against erosion. Petrol grease-up oil is a fake hydrocarbon, which has worldwide grease-up oil than higher temperature consumption

solidity. International Standards Organization (ISO) Viscosity Grade 32 (VG 32) oil describes the oil. The observed characteristics of the turbine-greasing oils are largely typical. Table IV presents a list of the oil's proposed attributes [27].

Table 2
 Characteristics of White metal Babbitt alloys [1]

Properties	Named Alloy	Modulus Young, GPa	Yield Strength, MPa	Ratio Poisson	Density, G/M ³	Range of Melting, °C
Value	Whiten Metal	50.01-50.39	120-124	0.3-0.21	7.17-7.27	238-339

Table 3
 Groove and pad measurements in millimeters

Properties	Arc Pad Length	Thickness of Pad	Layer of Copper Alloy	Density of Copper Alloy	White Metal Thickness	Pad Width	Depth of Beat	Width of Beat	The Groove's Width	Base Width
Value	44°	42.64	4.4	4.24	159	1.14	3.43	2.46		

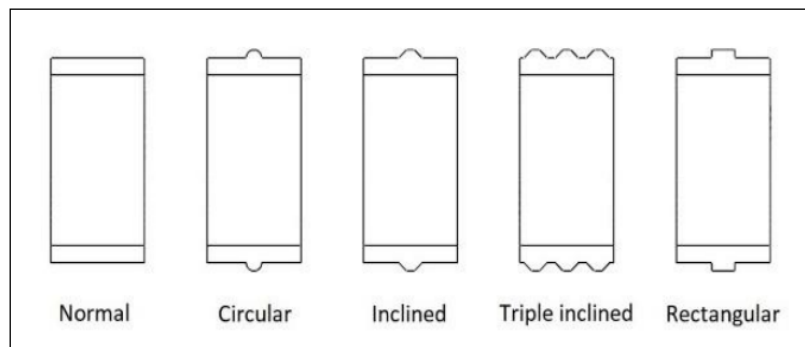


Fig. 11. Cross section of the groove tile pad bearing, [28]

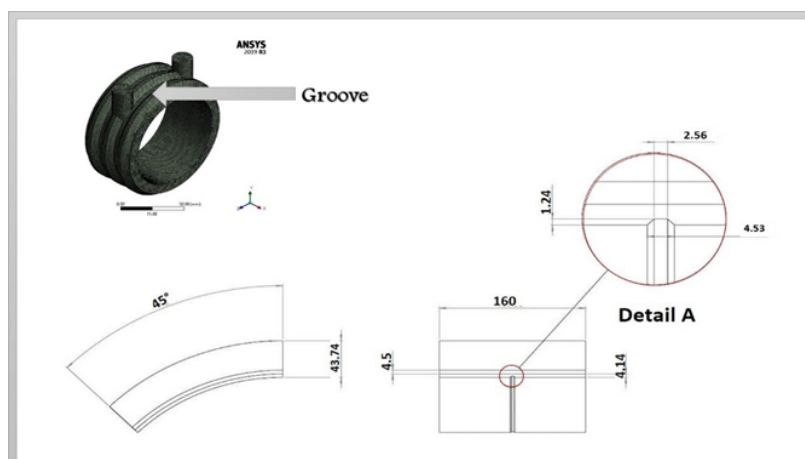


Fig. 12. The groove tile pad bearing's measurements and shape

Table 4
 Suggested the oil qualities

Properties	Density At 20°C G/Cm ³	Particular Gravity At 20°C	Viscosity At 40°C (Cst)	Viscosity At 100°C (Cst)	Acidity Mg Koh/G	Water Content (Ppm)	Flash Point Coc°C
Value	0.8403	0.8414	30.54	5.2	0.01	32	215

Subsequently, after making these previously mentioned upgrades, the strain was expanded to 1.5 bar, and the examination cycle was led in the Ansys based on these enhancements.

5.2.1 Free vibration

The findings of the modal analysis performed on a gas turbine with a given geometry were as follows: Figure 13 depicts the total deformation of 0.656 mm for the first mode at frequency 12.77 Hz, and Figure 14 displays the total deformation of 1.085 mm for the second mode at frequency 49.88 Hz.

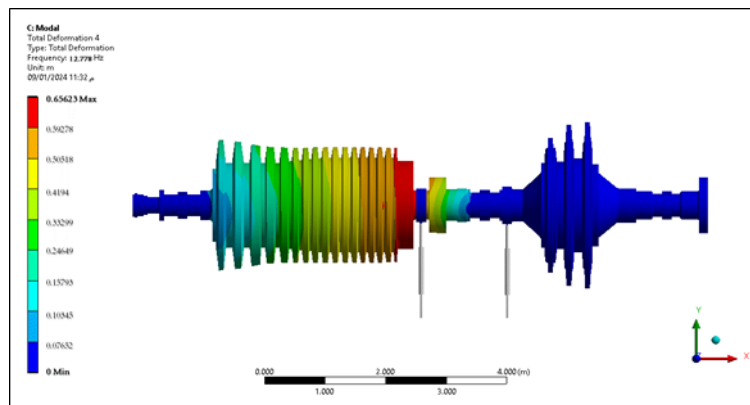


Fig. 13. Deformation of frequency 12. Hz.1st

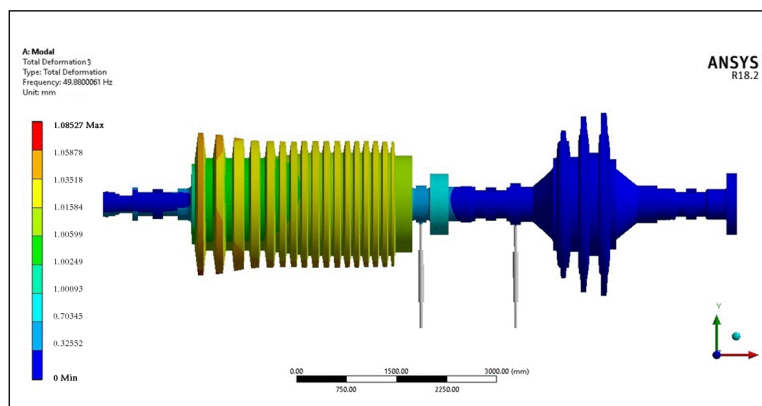


Fig. 14. The Deformation at frequency 49.88 Hz. 2nd

5.2.2 Transient analysis

Figure 15 exhibits the 1.253 mm overall deformation. The system reached stability 25.72 seconds, as shown in Figure 16, which reveals the abundance of deformation change with the time at its maximum amount. Figure 17 illustrates the strain value of 0.0047 for the material with an analogous

elastic modulus, whereas Figure 18 shows the stress value of 680.6 MPa obtained using the Von Mises technique for the same material.

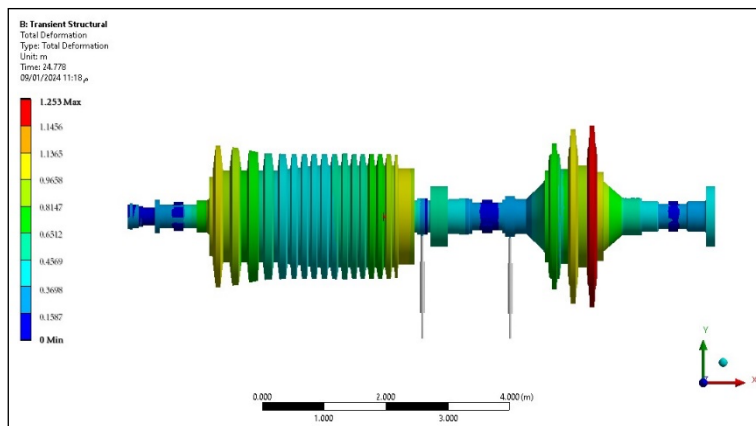


Fig. 15. Transient structure (Total deformation)

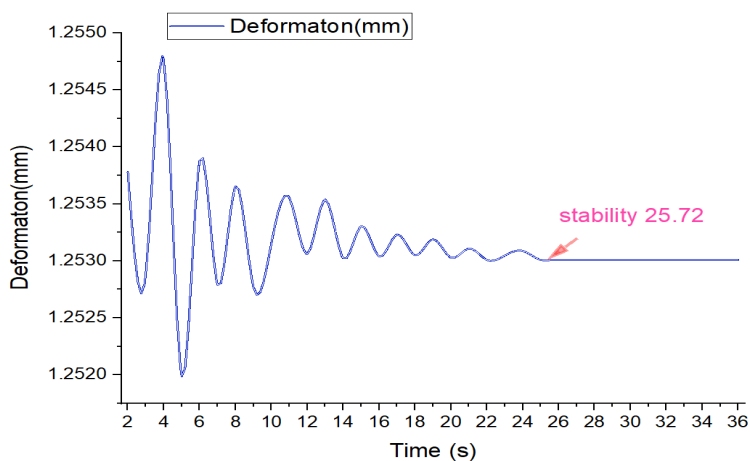


Fig. 16. Time affecting the deformation's amplitude value

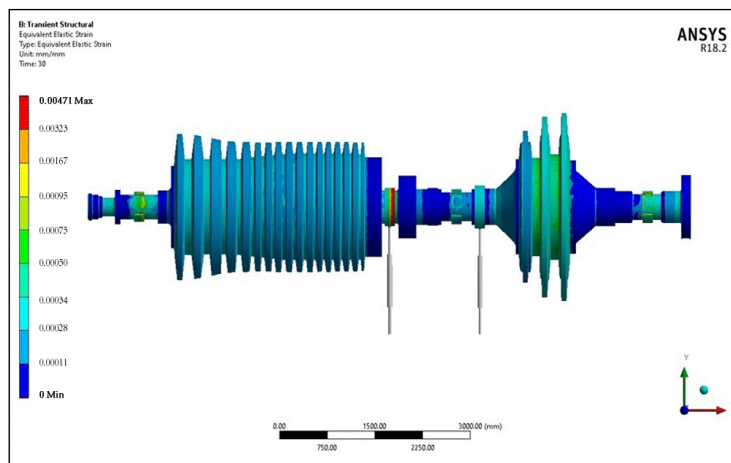


Fig. 17. Equivalent elastic modulus material (the strain value)

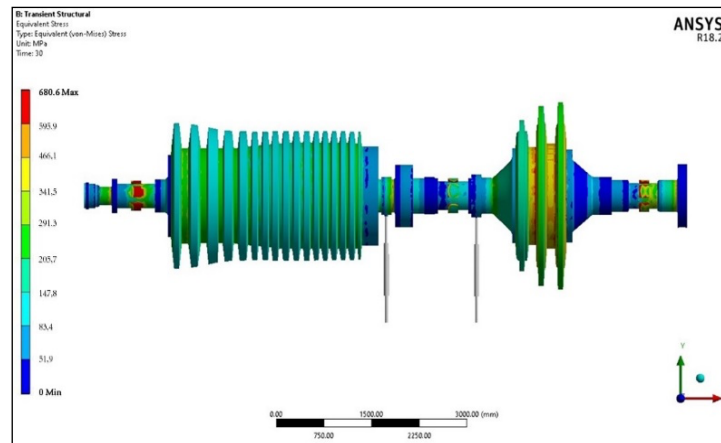


Fig. 18. The value of stress for comparable material as determined by the Von Mises Technique

5.2.3 Harmonic analysis (forced vibration)

At a frequency of 50 Hz, Figure 19 evinces the harmonic response's total deformation of 1.386 mm. And, Figure 20 indicates that maximum amount of amplitude is 1.368 mm, where the frequency is 50 Hz. Table V lists the results of comparison of the gas turbine system before development (B.D.) and after development (A.D.).

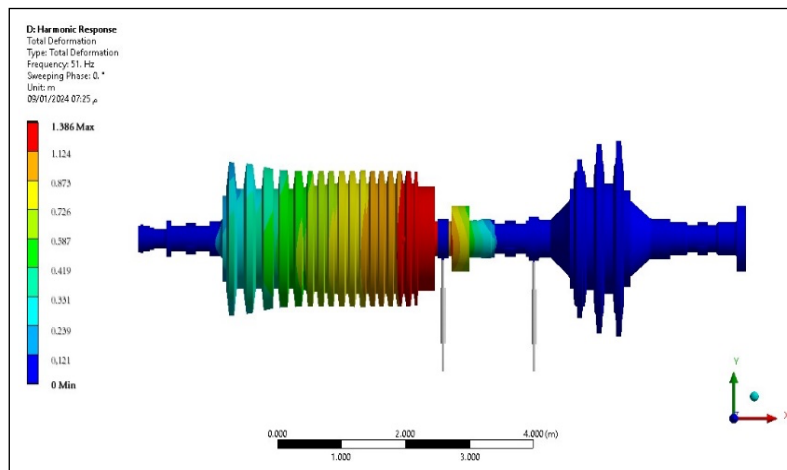


Fig. 19. Response of harmonic vibration at 50 Hz frequency

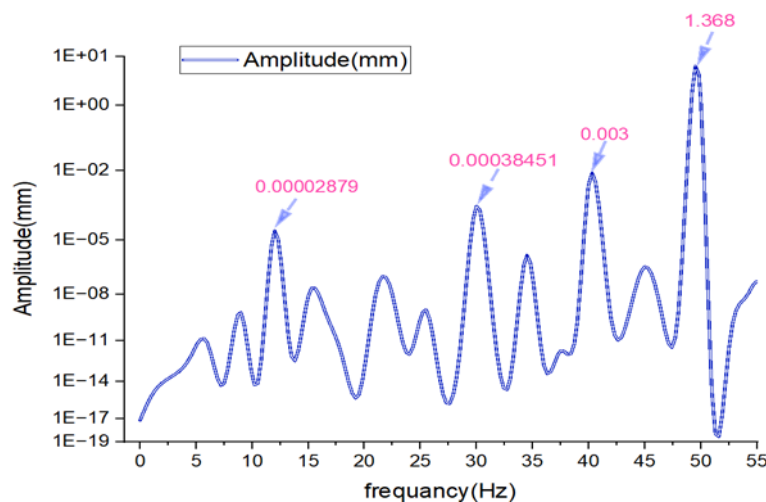


Fig. 20. The vibration value's amplitude with frequency

Table 4
Suggested the oil qualities

The Analysis Modal			Transient Analysis			Harmonic Analysis		
Deformation In 12.77 Hz.1 st	Deformation In 50 Hz.2 nd	Stability Time	Total Deformation	Equivalent Elastic Stress	Equivalent Elastic Strain	Deformation at Frequency 50 Hz	Amplitude of Vibration	
B.D	1.3124	(2.8891) mm	(53.52) sec	(2.238) mm	(1128) Mpa	0.0122	(2.2) mm	(2.3) mm
A.D	0.656	1.085	29.2 sec	1.253 mm	680.6 Mpa	0.0047	1.36 mm	1.368 mm

5. Conclusions

In this work, the dynamic examination framework model MS9001E for the gas turbine improvement was executed by utilizing scientific reproduction (Ansys programming). Upon examining the results of the two cases, the following deduction was made: In the analysis of model, the twisting value of the principal mode at recurrence (12 Hz) decreased to (0.656 mm) from its value of (1.3124 mm) prior to the improvement; this will reduce the weight on the framework, where an excitation capability links with the design's normal recurrence. This type of inquiry is used for the transient assessment to ascertain a design's strong response to each broad time-subordinate load. Following the improvements, a framework dependability time decreased to 29.2 sec. After the improvements, the system's deformation value decreased to 46.17%, the stress value reduced to 39.66%, and the strain value decreased to 61.47%. In the consonant, a reduction in these values indicates that the gas turbine is less likely to fail, leading to improved reliability. Also, the result manifested that the gas turbine's performance has improved, as it can now withstand higher loads and stresses reducing the vibrations emphasis on the rotor as well as the shaft-disk-blade.

Acknowledgement

This research was not funded by any grant.

References

- [1] Kadhim, Hayder Jawad, Thu'alaqir J. Kadhim, and Mohammed H. Alhwayzee. "A comparative study of performance of Al-Khairat gas turbine power plant for different types of fuel." In *IOP Conference Series: Materials Science and Engineering*, vol. 671, no. 1, p. 012015. IOP Publishing, 2020. <https://doi.org/10.1088/1757-899X/671/1/012015>
- [2] Mahroug, Youcef, Belgacem Said Khaldi, Mouloud Guemana, Ahmed Hafaifa, Abdelhamid Iratni, and Ilhami Colak. "ARMAX-based identification and diagnosis of vibration behavior of gas turbine bearings." *Diagnostyka* 24, no. 3 (2023). <https://doi.org/10.29354/diag/171277>
- [3] Salnikov, A. F., S. V. Bochkarev, and I. Zubko. "Experimental and theoretical studies of the influence of the bench elements on the transient operation of the turbine." *Ann Math Phys* 6, no. 1 (2023): 029-035. <https://doi.org/10.17352/amp.000073>
- [4] Abdulah, Alaa Jasim, Muhannad Z. Khalifa, and Abdul Jabbar Owaid. "Comparative Analysis of Two Alloys (GTD-111 and IN-738) used in Blade of Gas Turbine Model MS9001E at South Baghdad Station." In *Journal of Physics: Conference Series*, vol. 1973, no. 1, p. 012035. IOP Publishing, 2021. <https://iopscience.iop.org/article/10.1088/1742-6596/1973/1/012035/meta>
- [5] Oliveira, Marcus Vinicius Medeiros, and Gregory Bregion Daniel. "Vibrational signature of journal bearing oil starvation considering thermal effects and rotor unbalance variation." *Tribology International* 191 (2024): 109132. <https://doi.org/10.1016/j.triboint.2023.109132>
- [6] Xiong, Huiying, Yiheng Peng, Yiyang Hu, Lin Zhang, and Ying Li. "Vibration fault signal analysis and diagnosis of flue gas turbine." *Engineering Failure Analysis* 134 (2022): 105981. <https://doi.org/10.1016/j.engfailanal.2021.105981>
- [7] Mishra, Santwana, and Shipra Aggarwal. "A review of performance of textured journal bearing." *Tribology Online* 18, no. 7 (2023): 494-507. https://doi.org/10.1007/978-981-99-3844-5_27
- [8] Fernandez, Daniel Armando Pinilla, Blanca Foliaco, Ricardo Vasquez Padilla, Antonio Bula, and Arturo Gonzalez-Quiroga. "High ambient temperature effects on the performance of a gas turbine-based cogeneration system with

- supplementary fire in a tropical climate." *Case Studies in Thermal Engineering* 26 (2021): 101206. <https://doi.org/10.1016/j.csite.2021.101206>
- [9] Akhtar, Muhammad, Muhammad S. Kamran, Nasir Hayat, Anees Ur Rehman, and Awais A. Khan. "High-vibration diagnosis of gas turbines: An experimental investigation." *Journal of Vibration and Control* 27, no. 1-2 (2021): 3-17. <https://doi.org/10.1177/1077546320923917>
- [10] Rahmoune, Mohamed Ben, Ahmed Hafaifa, Abdellah Kouzou, XiaoQi Chen, and Ahmed Chaibet. "Gas turbine monitoring using neural network dynamic nonlinear autoregressive with external exogenous input modelling." *Mathematics and Computers in Simulation* 179 (2021): 23-47. <https://doi.org/10.1016/j.matcom.2020.07.017>
- [11] Fahmi, Al-Tekreeti Watban Khalid, Kazem Reza Kashyzaadeh, and Siamak Ghorbani. "A comprehensive review on mechanical failures cause vibration in the gas turbine of combined cycle power plants." *Engineering Failure Analysis* 134 (2022): 106094. <https://doi.org/10.1016/j.engfailanal.2022.106094>
- [12] Benyounes, A., A. Iratni, A. Hafaifa, and I. Colak. "A comparative investigation of modeling and control approaches for gas turbines: fuzzy logic, neural network and ANFIS." *International Journal of Smart Grid* 7, no. 2 (2023): 89-101.
- [13] MOHAMMED, Abubakar Kandi, Idris Ozigi, and Nasir Muhammed Lawal. "Gas Turbine Bearing Temperature Monitoring via Regression Modelling." *ABUAD Journal of Engineering Research and Development (AJERD)* 6, no. 1 (2023): 76-87. <https://doi.org/10.53982/ajerd.2023.0601.10-j>
- [14] Najjar, Yousef SH, Osama FA Alalul, and Amer Abu-Shamleh. "Degradation analysis of a heavy-duty gas turbine engine under full and part load conditions." *International Journal of Energy Research* 44, no. 6 (2020): 4529-4542. <https://doi.org/10.1002/er.5229>
- [15] A J Sriganapathy, Kiruthika B, Sopika.S, Sujithra.H, Yamuna R, "Esign And Analysis Of Thermalbarrier Coating On Gasturbineblade," nternational Advanced Research Journal in Science, Engineering and Technology, Vol. 9, Issue 6, June 2022. <https://doi.org/10.17148/IARJSET.2022.9606>
- [16] Mansoor, Hussein I., Mohsin Al-Shammari, and Amjad Al-Hamood. "Theoretical analysis of the vibrations in gas turbine rotor." In *IOP Conference Series: Materials Science and Engineering*, vol. 671, no. 1, p. 012157. IOP Publishing, 2020. <https://doi.org/10.1088/1757-899X/671/1/012157>
- [17] Abdulah, Alaa Jasim, Muhannad Z. Khalifa, and Abdul Jabbar Owaid. "Numerical analysis for determination of the vibrations and other parameters of the first stage blade of the gas turbine model (MS9001E)." In *AIP Conference Proceedings*, vol. 2415, no. 1, p. 060008. AIP Publishing LLC, 2022. [10.1063/5.0093071](https://doi.org/10.1063/5.0093071)
- [18] Shahriari, Behrooz, and Nedasadat Seddighi. "Stress analysis of non-linearly variable thickness rotating disk in gas turbine engine using hyper-geometric method." *Journal of Simulation and Analysis of Novel Technologies in Mechanical Engineering* 15, no. 2 (2023): 37-51. https://journals.iau.ir/article_704423.html
- [19] Inyang, Udeme Ibanga, Ivan Petrunin, and Ian Jennions. "Diagnosis of multiple faults in rotating machinery using ensemble learning." *Sensors* 23, no. 2 (2023): 1005. <https://doi.org/10.3390/s23021005>
- [20] Verbovyi, Anton Yevhenovych, Vladyslav Volodymyrovych Khomenko, C. Neamtu, V. Pavlenko, Vitalii Iovych Symonovskiy, and Ivan Volodymyrovych Pavlenko. "Rotor dynamics of turbocompressor based on the finite element analysis and parameter identification approach." (2022). [https://doi.org/10.21272/jes.2022.9\(2\).d1](https://doi.org/10.21272/jes.2022.9(2).d1)
- [21] Abdulah, Alaa J., Muhannad Z. Khalifa, and Abdul Jabbar O. Hanfesh. "Reducing vibrations generated in a gas turbine model MS9001E used in south baghdad power plant station by improving the design of bearings with damper." *Engineering and Technology Journal* 39, no. 09 (2021): 1454-1462. <https://doi.org/10.30684/etj.v39i9.2134>
- [22] Elwardany, Mohamed, Abd El-moneim M. Nassib, and Hany A. Mohamed. "Comparative evaluation for selected gas turbine cycles." *International Journal Of Thermodynamics* 26, no. 4 (2023): 57-67. <https://doi.org/10.5541/ijot.1268823>
- [23] Romanov, A. E., A. L. Kolesnikova, and M. Yu Gutkin. "Elasticity of a cylinder with axially varying dilatational eigenstrain." *International Journal of Solids and Structures* 213 (2021): 121-134. <https://doi.org/10.1016/j.ijsolstr.2020.12.010>
- [24] Gupta, Pradeep K. "Minimum energy hypothesis in quasi-static equilibrium solutions for angular contact ball bearings." *Tribology Transactions* 63, no. 6 (2020): 1051-1066. <https://doi.org/10.1080/10402004.2020.1788195>
- [25] E. Method, Buckling "Analysis for Wind Turbine Tower," Design: 2020.
- [26] Liu, Wing Kam, Shaofan Li, and Harold S. Park. "Eighty years of the finite element method: Birth, evolution, and future." *Archives of Computational Methods in Engineering* 29, no. 6 (2022): 4431-4453. <https://doi.org/10.1007/s11831-022-09740-9>
- [27] Abbood, Ahmed Imad, and Fadhel Abbas Abdulla. "Numerical investigation on the vibration reduction of rotating shaft using different groove shapes of tilt bearing." *Diagnostyka* 24 (2023). <https://doi.org/10.29354/diag/168084>